SAND2019-6568C

Differential Analysis of the Angle of Incidence Response of Utility-Grade PV Modules

Bruce H. King and Charles D. Robinson

Sandia National Laboratories, Albuquerque, NM, 87185-0951, USA

Abstract — Anti-reflective coatings (ARCs) are commonly applied to commercial modules to reduce reflection losses and improve energy harvest. Relative performance at low incidence angle is often indistinguishable between different modules and it is only at high incidence angle that performance becomes differentiated. It is also precisely in this range that accurate measurements are the most difficult to obtain, complicating efforts to compare the benefits of different coatings. In this study, the performance of multiple commercial modules with different coatings were compared. A differential approach was employed, facilitating relative comparisons between test devices and a common reference. Using this method, performance differences at high incidence angles could be visualized and quantified. Differential analysis was extended to multiple system performance models in order to predict and quantify potential improvements in annual energy harvest. Improvements were observed upwards of 1% seasonally and 0.5% annually for the best performing coatings. 10° fixed tilt systems were seen to potentially benefit the most from ARCs, while single axis trackers benefitted the least.

***Index Terms* — angle of incidence, diffuse irradiance, incident angle modifier, outdoor testing, PV modules, ARC**

I. Introduction

The angle of incidence response of a photovoltaic module describes its light gathering capability when incident sunlight is at an orientation other than normal to the module's surface. At low incident angles most modules have similar responses, while at increasing incident angles reflective losses dominate response and relative module performance becomes differentiated. Relative performance in this range is important for understanding the behavior of anti-reflective coatings (ARCs) designed to improve the light harvesting capability of modules and the potential power output of utility-scale photovoltaic systems. Angle of incidence (AOI) response is accounted for in power performance models by a unitless Incident Angle Modifier (IAM) [1] or AOI function such as $f_2(\theta)$ [2].

Angle of incidence response can be measured both indoors on a simulator or outdoors under natural sunlight [3]. Indoor measurements are typically made using either a minimodule or a single cell in a full-size module that has been electrically isolated. Indoor measurements promise to be more repeatable but require a collimated light source and are sensitive to uniformity of the light source. These methods are not practical to apply to monolithic thin film or glass-glass modules. Outdoor measurements can accommodate full size modules of any type and avoid concerns about the uniformity of light. However, measurements must be made opportunistically during favorable weather conditions. In either case, accurate measurement at high incidence angles can be problematic and create large uncertainty in the reported values.

Recently, Sandia demonstrated the capability to characterize up to eight utility-scale modules simultaneously outdoors. The test platform, a two-axis azimuth-elevation solar tracker, is shown below in Figure 1. Four commercially available 72-cell crystalline silicon modules are mounted on the right arm and four thin film cadmium telluride modules are mounted on the left arm. Several of the modules were known to feature anti-reflective coatings, while for others, this was unknown.

In this paper, the relative performance of select modules is compared to a plain glass module with no ARC using a simple differential method. This comparison is extended to performance predictions for three common system orientations, 10° and 35° fixed tilt and single axis tracking. Performance prediction comparisons include only the influence of off-axis reflective properties and do not include other module-to-module variations arising from factors such as solar spectrum, diode factor or cell temperature. These comparisons also do not include improvement in normal incident angle response imparted by ARCs.

Fig. 1. Eight PV modules tested simultaneously on a two-axis tracker

TABLE I
MODULE DESIGNATIONS

Identifier	Description	SNL ID
Mod1	Commercial, no ARC	3262
Mod2	Commercial, unknown ARC	3268
Mod3	Commercial, unknown ARC	3267
ARC1	Commercial, experimental ARC	3261

II. Experimental Procedure

Angle of incidence characterization was performed following the methods described in [4]. The procedure uses an Azimuth-Elevation solar tracker capable of rotating the test plane to solar incident angles between 0° and 90°. Solar irradiance during

Sandia National Laboratories is a multimission laboratory managed and operated by National Technology & Engineering Solutions of Sandia, LLC, a wholly owned subsidiary of Honeywell International Inc., for the U.S. Department of Energy's National Nuclear Security Administration under contract DE-NA0003525.

characterization was measured using two instruments, diffuse plane of array irradiance (E_{diff}) and direct normal irradiance (E_{DNI}). E_{diff} was measured using a global pyranometer equipped with a vertical shade band and installed on the test tracker [5] while E_{DNI} was measured with a pyrheliometer mounted on a separate weather tracker. Module electrical performance was monitored during the test using a conventional current-voltage (I-V) sweep system. Module temperature was monitored using three PT-100 RTD's adhered to the module back sheet.

TABLE II
ENVIRONMENTAL CONDITIONS DURING AOI CHARACTERIZATION

Condition	**4/15/18**	**4/18/18**	**4/26/18**
Ambient Temp, °C	16.9	15.5	23.9
Wind Speed, m/s	2.5	2.2	6.2
Relative Humidity, %	9.6	5.4	6.6
DNI, W/m²	1044	1053	1012
GNI, W/m²	1106	1132	1101
DNI/GNI	0.94	0.93	0.91
Air Mass	0.92	0.92	0.89

Characterization was performed near solar noon under clear sky conditions. Test dates and environmental conditions during testing are shown above in Table II. The tracker was dwelled for several minutes at predetermined angles in order to collect 4 to 5 IV curves per condition. *Isc* for analysis was extracted from each IV curve. Typical measured *Isc* for a test is shown in Figure 2.

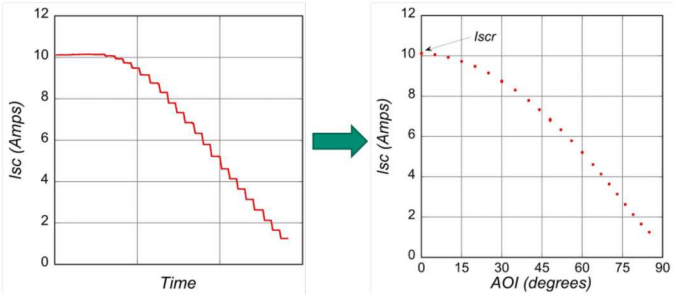

Fig. 2. Typical measured short circuit current as a function of time and angle of incidence. Multiple measurements at each angle are averaged for subsequent analysis. A reference condition at AOI=0, *Iscr*, is determined to normalize all remaining measurements.

Incident angle response is found by first correcting the measured *Isc* for temperature and optionally, spectrum.

$$I_{sc,Tr,AM1.5} = \frac{I_{sc}}{f_1(AM)[1+\hat{\alpha}_{Isc}[T_c - T_0]]}$$

A reference condition, I_{scr}, is then found at 0° incident angle.

$$I_{scr} = \frac{1}{n}\sum\left[I_{sc,Tr,AM1.5}\left[\frac{E_0}{E_{DNI}+E_{diff}}\right]\right]_n \quad @\ AOI = 0°$$

Normalized *Isc* (*Nisc*) is then found by removing cosine losses from each measured value and normalizing by *Iscr*.

$$Nisc = \left[\frac{E_0}{E_{DNI}\cos\theta}\right]\left[\frac{I_{sc,Tr,AM1.5}}{I_{scr}} - \left[\frac{G_{diff}}{G_0}\right]\right]$$

Multiple measurements obtained at each incident angle were then averaged and tabulated. The standard deviation of the averaged measurements in general was less than 0.5% and typically was less than 0.2%. The resulting normalized values may then be either tabulated or used to determine coefficients for a mathematical model. Whichever path is taken, the result is a unitless $f_2(\theta)$ function used for performance modeling.

It should be noted that the reference condition *Iscr* is analogous to, but typically different from *Isco*, measured under STC conditions. Use of an in-situ derived reference condition ensures the resulting function is both unitless and of unity value at AOI = 0°. It further enables the spectral or airmass correction to be ignored during the analysis provided that spectrum does not change appreciably during the test.

A typical set of responses for one day are shown below in Figure 3. All modules were seen to be relatively flat (pure cosine response) between 0° and ~55°. Beyond 55°, minor differences were apparent. Mod3 and ARC1 appear to be similar and consistently outperform all other commercial modules.

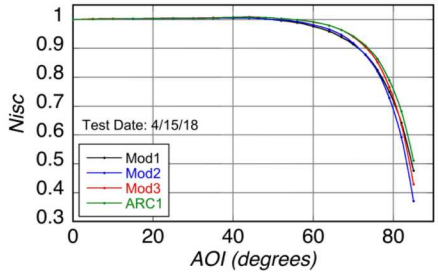

Fig. 3. Conventional Angle of Incidence Response of modules in this study

III. DIFFERENTIAL ANALYSIS

To further explore differences in performance, a differential analysis was performed on each module for each day of testing. Mod1, a plain glass module with no ARC coating was selected to serve as a common baseline case. The differential at each incidence angle was found by simply subtracting the *Nisc* value for this module from that of another module. Mathematically, the difference can be expressed as

$$\Delta Nisc = \left[\frac{E_0}{E_{DNI}\cos\theta}\right]\left[\left[\frac{I_{sc,Tr,AM1.5}}{I_{scr}}\right]_2 - \left[\frac{I_{sc,Tr,AM1.5}}{I_{scr}}\right]_1\right]$$

As with conventional analysis, the resulting values may be tabulated to create a unitless $\Delta f_2(\theta)$ function. The resulting differential is independent of diffuse light and is only dependent on DNI. One of the central challenges surrounding outdoor testing is accounting for the impact of diffuse light on the measured results. This finding may enable future testing

against well-calibrated reference devices. It is also important to point out that testing against a reference device should be performed simultaneously in order to minimize any differences arising from daily variation in atmosphere or tracker indexing. Finally, the analysis presented here assumes each module has identical diffuse utilization, which may not hold for all coatings.

The differential values were then plotted as a function of incidence angle, Figs. 4 and 5. Divergence from plain glass behavior can be seen as low as 30°. All modules showed a gain at higher AOI, to a peak after which the differential response rolls off. The degree of gain appears to be correlated with the angle at which the peak occurs. The differential for commercial modules Mod2 and Mod3 crossed over to negative values at high AOI, 70-80°, while ARC1 stayed positive and high after it started to roll off. Mod3 and ARC1 behaved similarly, with Mod3 showing slightly better performance at low incidence angles and ARC1 outperforming at very high angles. Visually, the repeatability across multiple days of testing appeared to be very good for ARC1, whereas Mod2 and Mod3 displayed more daily variation in differential response. It is possible that this behavior is related to module construction, as ARC1 and Mod1 (plain glass) share many construction similarities. Daily variation and the impact on predicted annual power will be addressed in more detail in Section V.

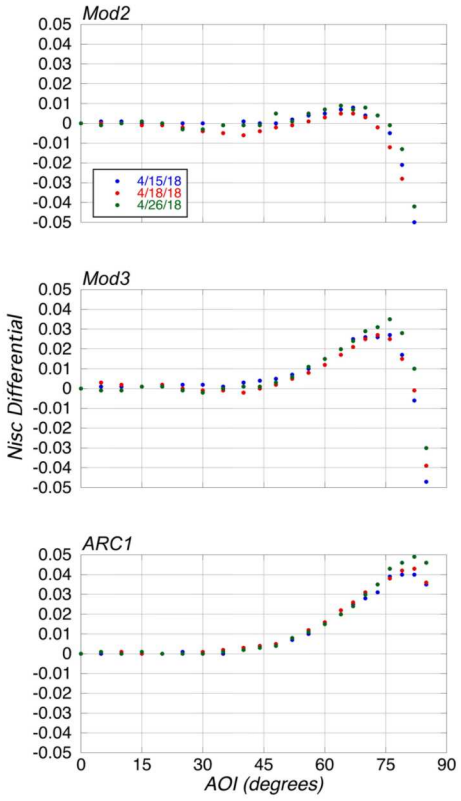

Fig. 4. Differential response of three modules relative to a plain glass module. Data presented is for individual tests on three different days under similar test conditions.

Differential response for each day was then averaged for each module. The average response of each module is plotted in Fig. 5. Here, the relative differences in response can clearly be seen. Mod3 and ARC1 lie almost on top of one another until diverging at high incidence angle, > 70°. Mod 2 diverges much lower, closer to 50°, where reflective losses typically begin to dominate cosine losses. Interestingly, Mod2 also displays a negative dip in differential response between ~ 20 – 50°. This dip will be seen to have a negative impact on predicted system performance in the following section.

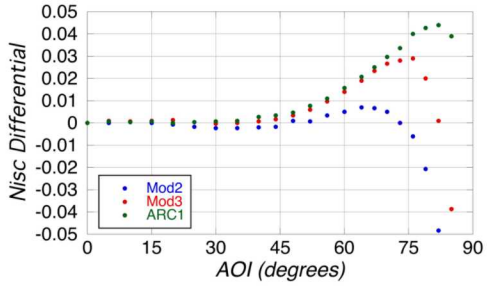

Fig. 5. Average differential response of three modules relative to a plain glass module.

IV. Application to PV System Performance

PV system performance modeling was conducted to investigate the applicability of differential response to understanding potential improvements in power generation. Differential response for each of the modules was applied to a range of fixed tilt orientations from 0° to 60° and a Single Axis Tracker (SAT). Fixed tilt arrays were oriented with an azimuth of 180° (due south) and single axis tracker was oriented with the rotation axis north to south. Module orientation on the tracker was flat relative to the torque tube. Backtracking and a ground coverage ratio of 0.33 were used.

To highlight the potential upper bound on the improvements in annual power generation, a one-year synthetic clear sky data set was generated for Albuquerque, NM for input to the model. Clear-sky functions from the Matlab version of PV_LIB (6) were used to used generate E_{DNI} and E_{GPOA} for each time step and array orientation. $\Delta f_2(\theta)$ was found using a lookup table of the averaged values and spline interpolation. Since this comparison sought only to evaluate power differences due to the reflective properties of modules, other factors affecting system performance such as spectrum and cell temperature were not included. Changes to the net effective irradiance were therefore directly proportional to differences in system power. A simplified version of a Performance Ratio calculation was used to normalize the calculated values and facilitate comparisons at different times of the year;

$$PR\ Gain = \frac{\sum_k \left[E_{DNI} \cos(\theta)[\Delta f_2(\theta)]\right]_k [time]_k}{\sum_k [E_{GPOA}]_k\ [time]_k}$$

As with determination of $\Delta f_2(\theta)$, this expression is independent of diffuse irradiance.

Daily results across one year for three common system orientations are shown in Figure 6. At 10° orientation, daily gains as high as 1% were realized for ARC1. Gains were more modest for Mod2, around 0.2%. Mod3 displayed performance gains that tracked ARC1, albeit not quite as high. Not surprisingly, peak gains were observed during the winter when sun elevation is low. Mod3 and ARC1 displayed significant gains throughout the year while gains vanished for Mod 2 module during the summer.

At 35° orientation, overall gains for Mod3 and ARC1 were not as pronounced as the 10° case. Here, peak gains of 0.3% and 0.4% were seen during the summer, matching that observed for the 10° case during the same time of year. Mod2 displayed almost no significant gain during any season.

Due to flat module orientation relative to the torque tube, results for the Single Axis Tracker resembled those observed for 10° Fixed Tilt, with the greatest gains occurring during the winter. However, the benefits of tracking systems are clearly seen as these gains largely vanish for all modules during the summer months.

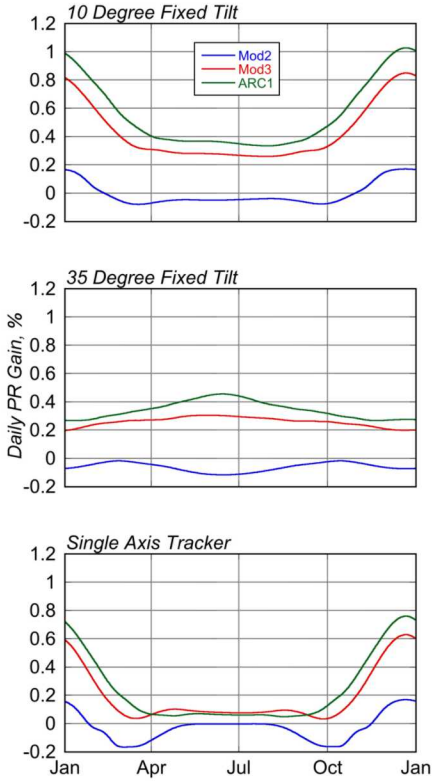

Fig. 6. Calculated Daily % gain for three system configurations (Albuquerque, NM).

Annual % Gain for a range of fixed tilt angles from 0° - 60° is shown below in Figure 7. As can be seen, Mod2 provides minimal gain in total energy relative to the plain glass module for any deployment scenario, and in fact may provide less energy overall. In contrast, Mod3 and ARC1 provide gains in all scenarios. The best annual gains occurred at sub-optimal orientations. Minimum benefit was realized at close to the optimal orientation of 35°, but still provided annual gains upwards of 0.25 - 0.35%.

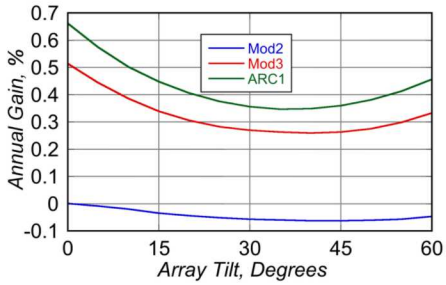

Fig. 7. Predicted Annual % Gain for three modules as a function of fixed tilt angle (Albuquerque, NM).

V. Uncertainty in Predicted Performance

While the differential results presented in Sections III and IV highlight compelling differences between each module, day to day variation in test results (e.g. Fig. 4) suggest that there could be significant variation in predicted differential performance depending on whether an individual or an average $\Delta f_2(\theta)$ function is used. To explore this variation, performance predictions were repeated using individual $\Delta f_2(\theta)$ functions from daily testing for 10°, 35° and SAT system configurations. Annual % Gain predictions are compared in Table II.

TABLE II
Predicted Annual % Gain for Individual and Average $\Delta f_2(\theta)$ Functions (Albuquerque, NM)

Module	Date	Orientation		
		10° Tilt	35° Tilt	SAT
Mod2	4/15/18	0.05	0.02	0.03
	4/18/18	-0.18	-0.19	-0.15
	4/26/18	0.07	-0.01	0.00
	Average	**-0.02**	**-0.06**	**-0.04**
	St Dev	**0.14**	**0.11**	**0.10**
Mod3	4/15/18	0.47	0.34	0.22
	4/18/18	0.31	0.20	0.12
	4/26/18	0.38	0.24	0.09
	Average	**0.39**	**0.26**	**0.15**
	St Dev	**0.08**	**0.07**	**0.07**
ARC1	4/15/18	0.48	0.34	0.17
	4/18/18	0.53	0.37	0.20
	4/26/18	0.49	0.33	0.17
	Average	**0.50**	**0.35**	**0.18**
	St Dev	**0.03**	**0.02**	**0.02**

Consistent with differential response, ARC1 demonstrated the lowest spread between maximum and minimum predicted annual % gain. The standard deviation was tight enough to provide high confidence that the predicted % gains relative to

the plain glass module are valid. The spread between predictions for Mod3 is significantly higher, however relative to the standard deviation, the predicted average gain is still significant. Mod2 demonstrated both the greatest spread and highest standard deviation. Given the low average gain combined with high uncertainty, it can be concluded that Mod2 demonstrates no measurable gain over the plain glass module.

Comparing Mod3 and ARC1, it can be concluded that ARC1 provides measurable benefit over Mod3 for the two fixed tilt orientations. However, while both provide benefit over plain glass for the single axis tracker scenario, the benefits of ARC1 over Mod3 largely vanish.

VI. Summary and Next Steps

A differential angle of incidence analysis method was developed to compare the potential improvement in module performance of various anti-reflective coatings relative to plain glass. The resulting differential is mathematically independent of diffuse irradiance, a long-standing source of uncertainty in angle of incidence testing. The method was applied to several commercial utility-grade modules and a non-commercial module with an experimental coating. Average differential response provided an effective way of visualizing the improvements in AOI performance due to advanced coatings. The experimental coating was seen to have the best performance. One of the commercial modules displayed significant improvement, similar to the experimental coating, while the other commercial module displayed only moderate improvement.

The differential analysis was extended to system performance modeling to demonstrate potential improvement in annual yield due to a coating. Sub-optimal system orientations (i.e. horizontal) stand to benefit the most from advanced coatings while optimized systems such as single axis trackers stand to benefit the least. Annual gains in performance as high as 0.35% absolute were observed for optimized fixed tilt orientations. By applying the differential method to predicted annual performance, it could be seen that the experimental coating provided a consistent 0.1% improvement over the better performing commercial module under all fixed tilt orientations but little to no gain in a tracking system. The lesser performing commercial module was seen to provide no significant benefit under any situation and may have in fact reduced annual energy relative to the plain glass module.

Uncertainty of the analysis method was assessed by comparing predictions using AOI functions measured on individual days against predictions from an averaged function. The module with the experimental coating was seen to have the least variation in response, followed by the better performing commercial module. The lesser performing commercial module displayed the greatest uncertainty, likely due to its' relatively low performance in the first place.

The module with the experimental coating was more similar in construction to the reference module than the two commercial modules, which may have contributed to its' low variation in performance. Otherwise, the potential sources of variation observed between different testing days are unknown. Sandia has commissioned construction of several custom full-size reference modules with plain glass for future testing to try to understand factors that may influence day-to-day variations in AOI response.

Acknowledgements

This material is based upon work supported by the U.S. Department of Energy's Office of Energy Efficiency and Renewable Energy (EERE) under Solar Energy Technologies Office (SETO) Agreement Number 34364. Sandia National Laboratories is a multi-mission laboratory managed and operated by National Technology and Engineering Solutions of Sandia LLC, a wholly owned subsidiary of Honeywell International Inc. for the U.S. Department of Energy's National Nuclear Security Administration under contract DE-NA0003525.

References

[1] N. Martin and J. M. Ruiz, "Calculation of the PV modules angular losses under field conditions by means of an analytical model," *Solar Energy*, Vol. 70, pp. 25-38, 2001.

[2] D. L. King, W. E. Boyson, J. A. Kratochvil, "Photovoltaic Array Performance Model,", Sandia National Laboratories, SAND2004-3535, 2004.

[3] IEC 61853-2:2016, "Photovoltaic (PV) module performance testing and energy rating – Part 2: Spectral responsivity, incident angle and module operating temperature measurements"

[4] Bruce H. King, Clifford W. Hansen, Dan Riley, Charles D. Robinson, Larry Pratt, "Procedure to Determine Coefficients for the Sandia Array Performance Model (SAPM)," SAND2016-5284, Sandia National Laboratories, Albuquerque, NM, 2016.

[5] B. H. King, D. Riley, C. Robinson and L. Pratt, "Recent Advancements in Outdoor Measurement Techniques for Angle of Incidence Effects," in *42nd IEEE Photovoltaic Specialist Conference*, 2015.

[6] PV_LIB Toolbox for MatLab Version 1.32. https://pvpmc.sandia.gov/applications/pv_lib-toolbox/matlab/